J Mater Sci: Mater Med (2008) 19:531–540
DOI 10.1007/s10856-007-3065-y

Sol–gel processing of drug delivery zirconia/polycaprolactone hybrid materials

Michelina Catauro · Mariagrazia Raucci · Giovanni Ausanio

Received: 2 March 2006 / Accepted: 12 May 2006 / Published online: 10 July 2007

Abstract Poly(ε-caprolactone) (PCL 6, 12 and 24 wt%) and zirconium (ZrO_2) organic–inorganic hybrid materials have been synthesized by the sol–gel method from a multicomponent solution containing zirconium propoxide [$Zr(OC_2H_7)_4$], poly(ε-caprolactone) (PCL), water, chloroform ($CHCl_3$). Sodium ampicillin was incorporate in the hybrid materials to verify the effect as local controlled drug delivery system. The structure of interpenetrating network is realized by hydrogen bonds between Zr-OH group (H donator) in the sol–gel intermediate species and carboxylic group (H-acceptor) in the repeating units of the polymer. The presence of hydrogen bonds between organic/inorganic components of the hybrid material was proved by FTIR analysis. The morphology of the hybrid material was studied by scanning electron microscope (SEM). The structure of a molecular level dispersion has been disclosed by atomic force microscope (AFM), pore size distribution and surface measurements. The bioactivity of the synthesized hybrid material has been showed by the formation of a layer of hydroxyapatite on the surface of PCL/ZrO_2 samples soaked in a fluid simulating the composition of the human blood plasma. Release kinetics in a simulate body fluid (SBF) have been subsequently investigate. The amount of sodium ampicillin released has been detected by UV–VIS spectroscopy and SEM. The release kinetics seems to occur in more than one stage. HPLC analysis has also been taken to ensure the integrity of ampicillin after the synthetic treatment.

M. Catauro (✉)
Department of Aerospace and Mechanical Engineering, Second University of Naples, Via Roma n°21, Aversa, CE 81031, Italy
e-mail: michelina.catauro@unina2.it

M. Raucci
Department of Materials and Production Engineering, University of Naples Federico II, Piazzale Tecchio, Naples 80125, Italy

G. Ausanio
INFM-Coherentia Department of Physics Science, University of Naples Federico II, Piazzale Tecchio, Naples 80125, Italy

Introduction

The study of organic–inorganic nanocomposites networks has recently become an expanding field of investigation [1, 2]. At first glance, these materials are considered as bi-phasic materials, where the organic and inorganic phase is mixed at the nm to sub-μm scales. Nevertheless, it is obvious that the properties of these materials are not just the sum of the individual contributions from both phases; the role of the inner interfaces could be predominant. The nature of the interface has been used recently to divide these materials into two distinct classes [3]. In class I, organic and inorganic compounds are embedded and only weak bonds (hydrogen, van der Waals or ionic bonds) give the cohesion to the whole structure. They result from much research work emerging from sol–gel and polymer chemists and these materials will present a large diversity in their structures and final properties. In class II materials, the phases are linked together through strong chemical bond (covalent or ionic-covalent bonds).

The sol–gel process has proved to be versatile and has been widely used in the preparation of organic/inorganic hybrid materials, [4–6] non-linear optical materials [7], and mesomoporous materials [8]. The sol–gel chemistry is based on the hydrolysis and polycondensation of metal alkoxides $M(OR)_x$, where M = Si, Sn, Zr, Ti, Al, Mo, V,

W, Ce and so forth. There is considerable interest in organic–inorganic hybrid composite materials prepared via the sol–gel process. A variety of organic polymers have been introduced into inorganic networks to afford the hybrid or composite materials with or without covalent bonds between the polymer and inorganic, components, respectively. The sol–gel reactions are affected by the value of many parameters such as structure and concentration of the reactants, solvents, and catalysts as well as reaction temperature and rate of removal of by-products and solvents [9, 10]. In particular the presence of organic components modifies the morphology and physical properties of the sol–gel products. For example, the base-catalyzed sol–gel reaction usually results in translucent or opaque products with visible organic–inorganic phase separation. Under acid catalysis and carefully controlled reaction conditions, transparent and monolithic hybrid/composite materials can be obtained.

A key issue that remains unresolved in these organic-modified materials is the degree of mixing of the organic–inorganic components, i.e., the phase homogeneity. The high optical transparency to visible light indicates that the organic–inorganic phase separation, if any, is on a scale of ≤400 nm. Many conventional methods for analyzing composite materials have not proved to be effective. For example, the changes in and disappearance of well-defined glass transition of the polymer component as measured by differential scanning calorimeter (DSC) or dynamic mechanical analysis (DMA) suggests the diminution of phase separation but offer little quantitative information [11, 12]. Transmission electron microscopy (TEM) often fails to provide useful morphological data because of weak contrast [11]. Recently, there have been several reports with encouraging examples of applying atomic force microscopy (AFM) in the analysis of sol–gel materials [11, 13].

In a previous paper [14, 15] a polycaprolactone/SiO_2, polycaprolactone/$CaO{\bullet}SiO_2$, hybrid material class I has been prepared via sol–gel process. The existence of the hydrogen bonds between organic/inorganic hybrid and the formation of a hydroxyapatite layer on the surface has been proved by FTIR analysis. The phase homogeneity was also studied using scansion electron microscopy (SEM) and atomic force microscopy (AFM).

It is known that ZrO_2 glass is bioactive, i.e. it is able to bond to living bone [16]**.** As reported in the literature **[**17, 18], the essential condition for glasses and glasses-ceramics to bond to living bone is the formation of a bone-like apatite layer on the surfaces. "In vitro" studies are (SBF) to study hydroxyapatite formation on the surface.

The aim of the present paper is the sol–gel synthesis, characterization and bioactivity of PCL/ZrO_2 hybrid materials. The release kinetics from the amorphous bioactive materials containing sodium ampicillin was analysed. The organic component was chosen taking into account the biodegradable and biocompatible nature of the poly(ε-caprolactone).

Experimental

Sol–gel synthesis

The hybrids inorganic/organic materials (PCL = 6, 12 and 24 wt%) were prepared by means of sol–gel process from an analytical reagent grade of zirconium propoxide $Zr(OC_3H_7)_4$, yttrium chloride YCl_3 in ethanol-acetylaceton-water mixture, polycaprolactone (PCL Mw = 65000) in chloroform as solvent.

Acetylaceton was also added to control the hydrolytic activity of zirconium alkoxide. The alcohol solution of YCl_3 was slowly added to the solution of $Zr(OC_3H_7)_4$ and then stirred with a magnetic stirrer.

Figure 1 shows the flow chart of hybrid synthesis by the sol–gel method. Molar ratio of the starting materials is indicated in the figure.

ZrO_2/PCL (PCL = 6, 12 and 24 wt%), all mixed with sodium ampicillin (Sigma-Aldrich). After the addition of each reactant the solution was stirred and the resulting sols were uniform and homogeneous. The time of gelification was 7 days. After gelation the gels were dried by air at 50 °C for 24 h to remove the residual solvent; this treatment does not modify the stability of ampicillin and small glassy pieces were obtained. Discs with a diameter of

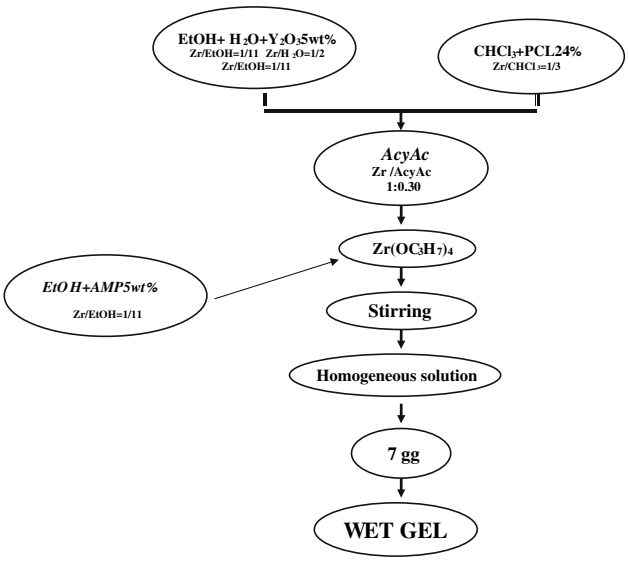

Fig. 1 Flow chart of PCL/ZrO_2-5 wt%Y_2O_3 gel synthesis

13 mm and a thickness of 2 mm were obtained by pressing a fine (<125 μm) gel powders into a cylindrical holder.

Chromatographic experiments were carried out on a Shimadzu HPLC system, equipped with a Class-VP 5.0 software, an UV spectrophotometric detector SPD-10AVvp and two pumps LC-10ADvp, with low-pressure gradient systems. Samples of solutions were injected by a syringe via a Rheodyne loop injector. The loop volume was 20 μL. The analytical column was a Phenomenex C_{18} (150 × 4.60 mm; 5 μ). The flow rate of the mobile phase A (water) was set at 0.8 mL/min and that of the mobile phase B (methanol) was set at 0.2 ml/min. The total run time was 10 min.

HPLC grade methanol was obtained by Sigma-Aldrich. HPLC grade water was prepared using a Millipore (0.22 μm) system.

A standard solution of ampicillin 3 mM in SBF was prepared and the samples were taken at the end of the release from the materials.

The nature of ZrO_2 gel, polycaprolactone (PCL) and PCL/ZrO_2 hybrid materials were ascertained by X-ray diffraction (XRD) analysis using a Philips diffractometer. Powder samples were scanned from $2\Theta = 5°$ to 60° using CuK_α radiation.

The presence of hydrogen bonds between organic/inorganic components of the hybrid materials was ascertained by FTIR analysis. Fourier transform infrared (FTIR) transmittance spectra were recorded in the 400–4000 cm^{-1} region using a Mattson 5020 system, equipped with a DTGS KBr (Deuterated Tryglycine Sulphate with potassium bromide windows) detector, with resolution of 2 cm^{-1} (20 scans). KBr pelletised disks containing 2 mg of sample and 200 mg KBr were made. The FTIR spectra were elaborated by Mattson software (FTIR Macros).

The microstructure of the synthesized gels has been studied by a scanning electron microscopy (SEM) Cambridge model S-240 on samples previously coated with a tin Au film and by a Digital Instruments Multimode atomic force microscopy (AFM) in contact mode in air.

Study in vitro bioactivity

In order to study their bioactivity, samples of the studied hybrid materials were soaked in a simulated body fluid (SBF) with ion concentrations, as reported elsewhere [18], nearly equal to those of the human blood plasma. During soaking the temperature was kept fixed at 37 °C. The ability to form an apatite layer was studied by submitting reacted samples to SEM and EDS analysis. Taking into account that [19–21] the ratio of the exposed surface to the volume solution influences the reaction, a constant ratio of 50 mm^2 ml^{-1} of solution, was respected as in Ref. 18. An electron microscope (Cambridge Stereo scan 240) equipped with an energy dispersive analytical system (EDS) LINK AN 10000 was used in order to verify the morphology of the coated sample and to perform a qualitative elemental analysis.

Study of in vitro release

For the study of ampicillin release, the discs of the investigated materials were soaked in 15 mL of SBF, continuously stirred, at 37 °C. The SBF was previously filtered with a Millipore (0.22 μm) system, avoiding bacterial contamination. Ampicillin release measurements were carried out by means of UV–VIS spectroscopy with a Shimadzu UV mini-1240. Absorbance values were taken at a wavelength λ = 197 nm, corresponding to the an absorbance maximum value.

The calibration curve, was determined by taking absorbance versus Sodium Ampicillin concentration between 0 and 3 mM as parameters. For this interval, the calibration curve fits the Lambert and Beers' law [22]:

$$A = 1.265 \times C,$$

where A is the absorbance and C is the concentration (mM).

Results and discussion

Gelation is the result of hydrolysis and condensation reactions according to the following reactions

$$Zr(OC_3H_7)_4 + nH_2O \Rightarrow Zr(OC_3H_7)_{4-n}(OH)_n + nC_3H_7OH \quad (1)$$

$$-ZrOH + CH_3O - Zr- \Rightarrow \equiv Zr - O - Zr \equiv + C_3H_7OH \quad (2)$$

$$\equiv Zr - OH + OH - Z \equiv r \Rightarrow \equiv Zr - O - Zr \equiv + H_2O \quad (3)$$

$$Y^{3+} + 3H - OZr \equiv \Rightarrow [Y(-OZr \equiv)_3] + 3H^+ \quad (4)$$

The reaction mechanism it is generally accepted to proceed through a second order nucleophic substitution [23].

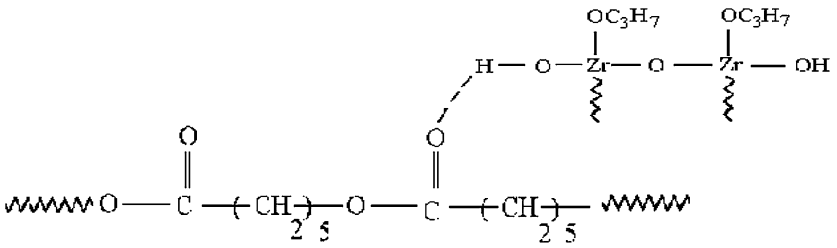

(5)

The reaction 5 shows the formation of hydrogen bond between the carbossilic group of organic polymer and the hydroxyl group of inorganic matrix.

Sol–gel characterization

FTIR spectroscopic analysis of Fig 2 (a) the ZrO_2-5 wt%Y_2O_3, and (b, c, d) PCL/ZrO_2-5 wt%Y_2O_3 (6, 12 and 24 wt%) gel showed that the characteristic peaks of PCL (2840-2928 cm^{-1} are attributed to the symmetric stretching of -CH_2- of polycaprolactone) appear in b,c,d.

The spectrum Fig 2 (b,c,d) also indicates a broad O-H stretching trasmittance at about 3,000-3,600 cm^{-1}, absent in ZrO_2-5 wt%Y_2O_3 (a).

The nature and the microstructure of the PCL/ZrO_2-5 wt%Y_2O_3 hybrid materials have been studied by X-ray diffraction (XRD), scanning electron microscopy (SEM) and atomic force microscopy (AFM).

The diffractograms in Fig.3 show that ZrO_2-5 wt%Y_2O_3 gel exhibits broad humps characteristic of amorphous materials, Fig. 3a, while sharp peaks can be detected on the diffractogram of polycaprolactone typical of a crystalline material, Fig. 3b. On the other hand the XRD spectrum of PCL/ZrO_2-5 wt%Y_2O_3 (PCL 6, 12 and 24 wt%) Fig. 3c,

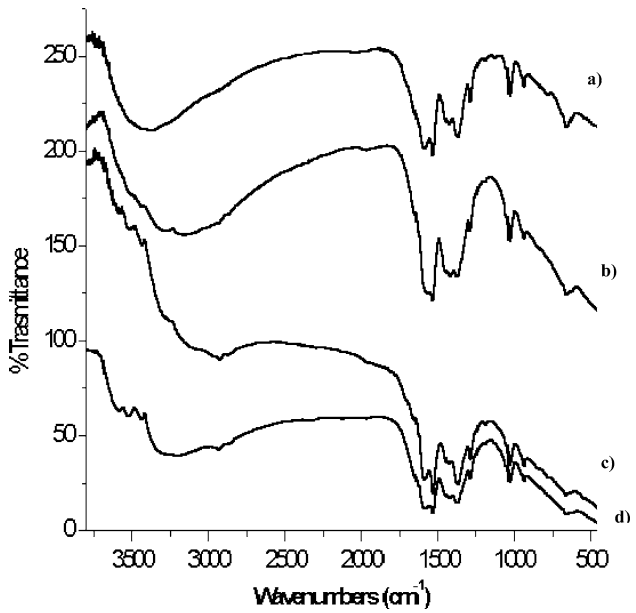

Fig. 2 FTIR of (**a**) ZrO_2 gel; (**b**) PCL/ZrO_2 gel 6 wt%; (**c**) PCL/ZrO_2-5 wt%Y_2O_3 gel 12 wt% and ZrO_2 gel 24 wt%

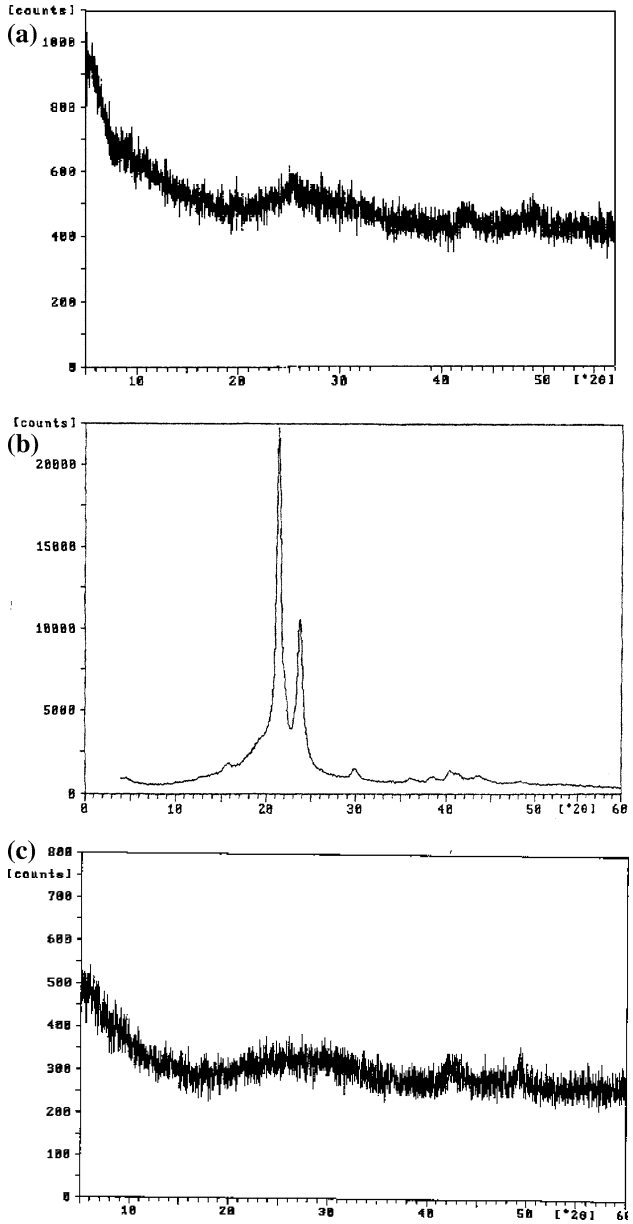

Fig. 3 XRD of (**a**) ZrO_2-5 wt%Y_2O_3 gel, (**b**) PCL and (**c**) PCL/ZrO_2-5 wt%Y_2O_3 gel 24 wt%

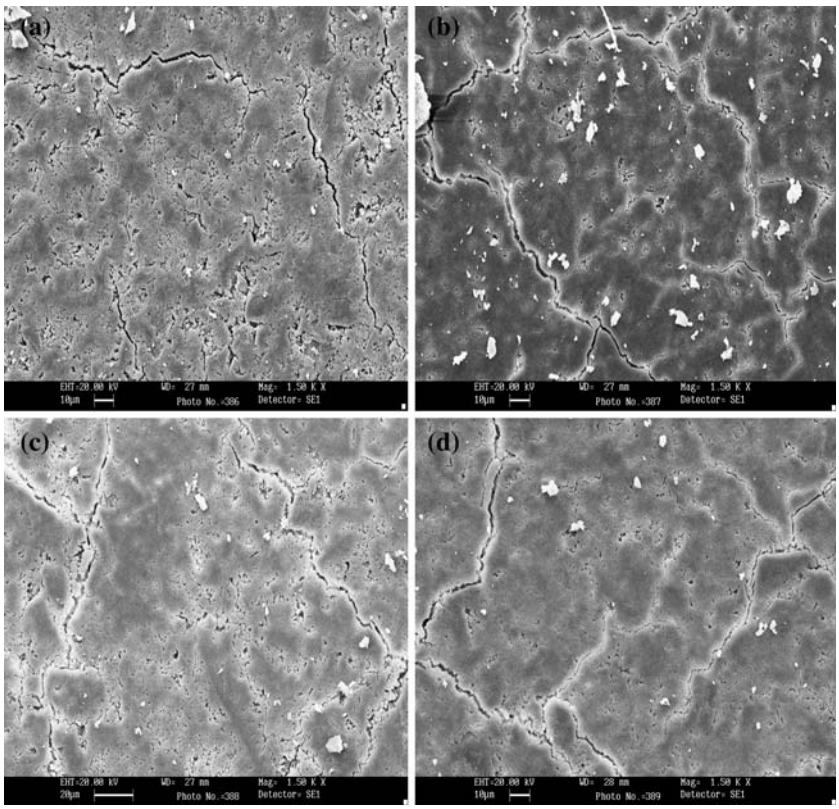

Fig. 4 SEM micrograph of ZrO_2-5 wt%Y_2O_3 gel

exhibits broad humps characteristic of amorphous materials is amorphous as well that of ZrO_2 gel.

SEM micrographs of a ZrO_2-5 wt%Y_2O_3 gel sample and of PCL/ZrO_2-5 wt%Y_2O_3 gel samples are shown in Fig. 4(a,b,c,d). No appreciable difference between the morphology of the four amorphous materials can be observed. The degree of mixing of the organic–inorganic components, i.e. the phase homogeneity has been ascertained applying the atomic force microscopy (AFM) in the analysis of the sol–gel hybrid materials.

The AFM contact mode image can be measured in the height mode or in the force mode. Force images (z range in nN) have the advantage that they appearing sharper and richer in contrast and that the contours of the nanostructure

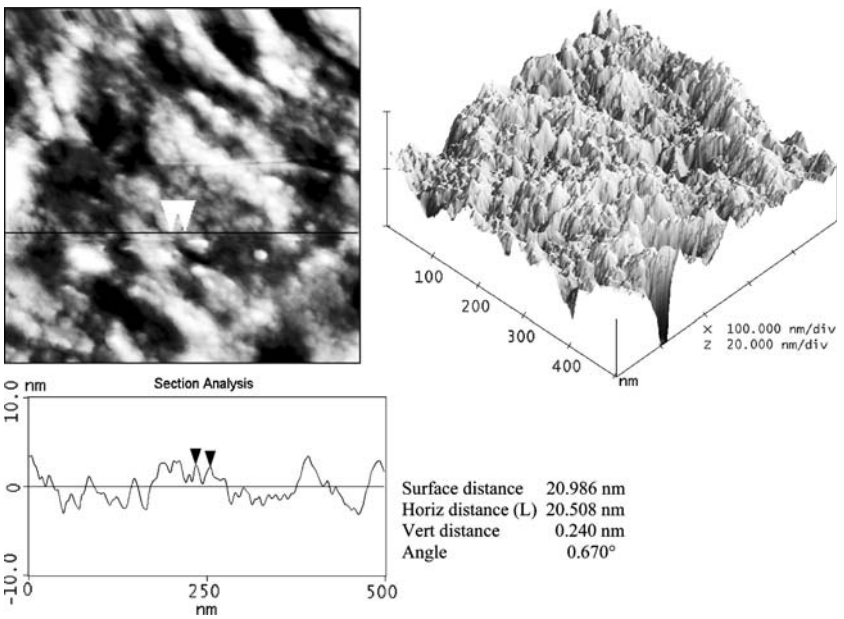

Fig. 5 AFM image showing the microstructure of ZrO_2-5 wt%Y_2O_3

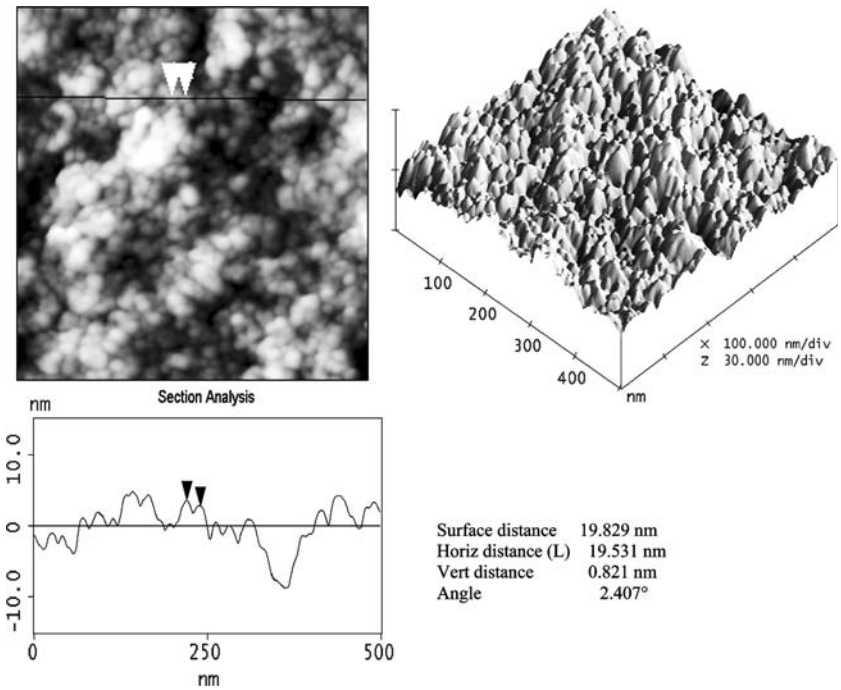

Fig. 6 AFM image showing the microstructure of PCL/ZrO_2-5 wt%Y_2O_3 gel 6 wt%

elements are clearer. Whereas, height images (z range in nm) show a more exact reproduction of the height itself [24]. In this work the height mode has been adopted to evaluate the homogeneity degree of the hybrid materials. The AFM topographic image of ZrO_2 and PCL/ZrO_2-5 wt%Y_2O_3 gels samples are shown in Figs. 5–8 respectively. As can be observed the average domain size are 21 nm for ZrO_2-5 wt%Y_2O_3 and 19 nm for PCL/ZrO_2-5 wt%Y_2O_3 (PCL 6, 12 and 24 wt%). This result confirms that the PCL/ZrO_2-5 wt%Y_2O_3 gel synthesized can be considered an organic/inorganic hybrid material as suggested by literature data [25].

A chromatographic analysis was carried out to ensure the integrity of the β-lactam ring of ampicillin, after the synthetic treatment. The conditions described in the experimental section allow to separate the two isomers of the antibiotic with retention times of 1.6 min and 2.2 min. All the materials, ZrO_2-5 wt%Y_2O_3 + PCL(6, 12 and

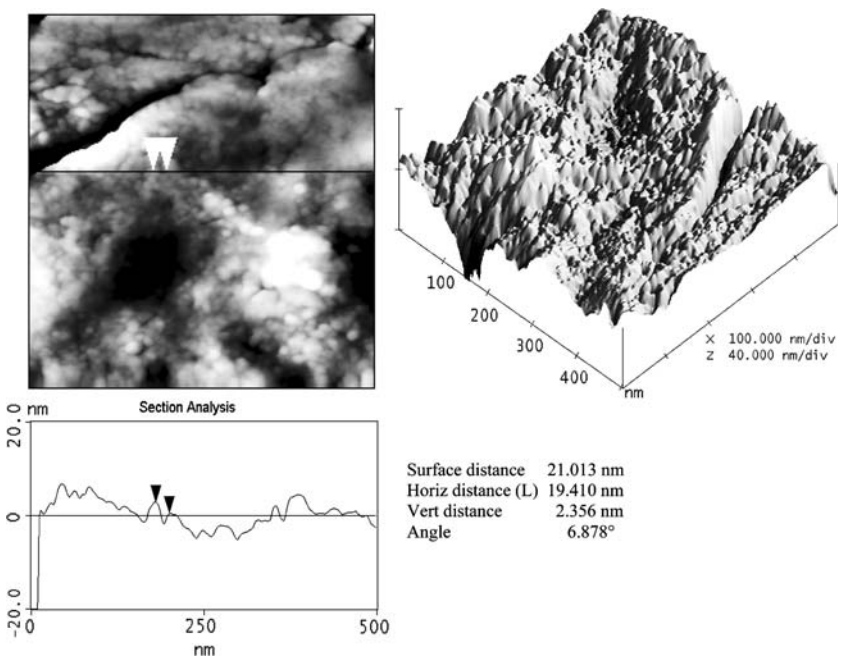

Fig. 7 AFM image showing the microstructure of PCL/ZrO_2-5 wt%Y_2O_3 gel 12 wt%

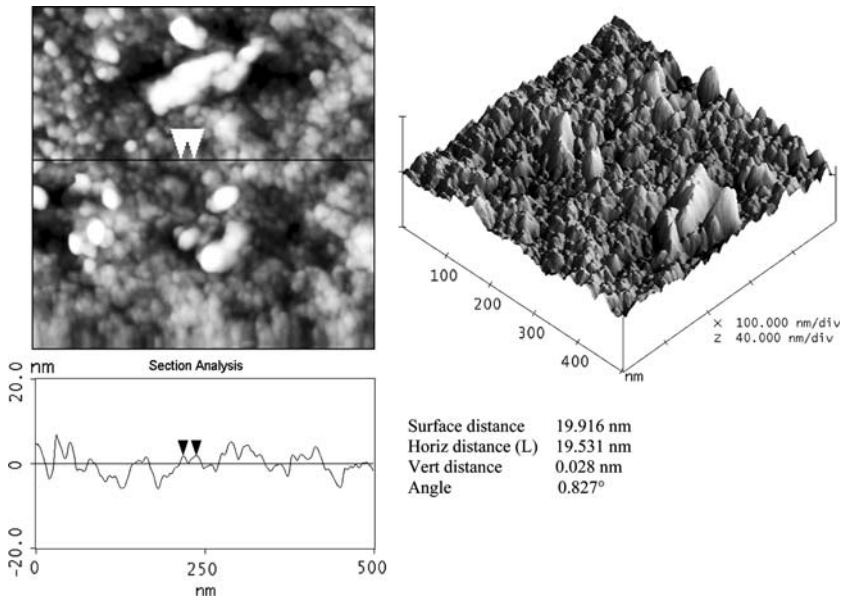

Fig. 8 AFM image showing the microstructure of PCL/ZrO_2-5 wt%Y_2O_3 gel 24 wt%

24 wt%) release ampicillin without any sign of decomposition, as demonstrated by the perfect superimposition of the samples chromatograms with that of a standard solution of ampicillin (data not shown).

SEM micrograph and EDS analysis

Moreover an evaluation of the morphology of the apatite deposition and a qualitative elemental analysis were carried out by electron microscopy observations on pelletised discs previously coated with a thin graphite film.

The hybrid materials were finally soaked in SBF, as indicated in Ref. 18, for "in vitro" bioactivity tests**.** Figures 9-11a show the SEM micrographs of a sample soaked in SBF for 21 days. The characteristic apatite globular crystals are clearly visible. As can be seen, the EDS reported in Figs. 9-11b confirm that the surface layer observed in the SEM micrographs is composed of calcium phosphate and which increases as the PCL (see table).

21 days after immersion in SBF	Contents of Ca atomic %	Contents of P atomic %
ZrO_2-5 wt%Y_2O_3 + PCL6 wt%	3.20	2.01
ZrO_2-5 wt%Y_2O_3 + PCL12 wt%	3.68	2.30
ZrO_2-5 wt%Y_2O_3 + PCL24 wt%	8.73	5.45

Release kinetics

Kinetic measurements of ampicillin release from the studied materials were carried out in 15.0 mL of SBF, incubated at 37 ± 0.1 °C and under continuous magnetic stirring at 150 rpm. Sink conditions were maintained throughout all studies. The discs used were obtained with particles size between 63–125 μm compressed at three tons

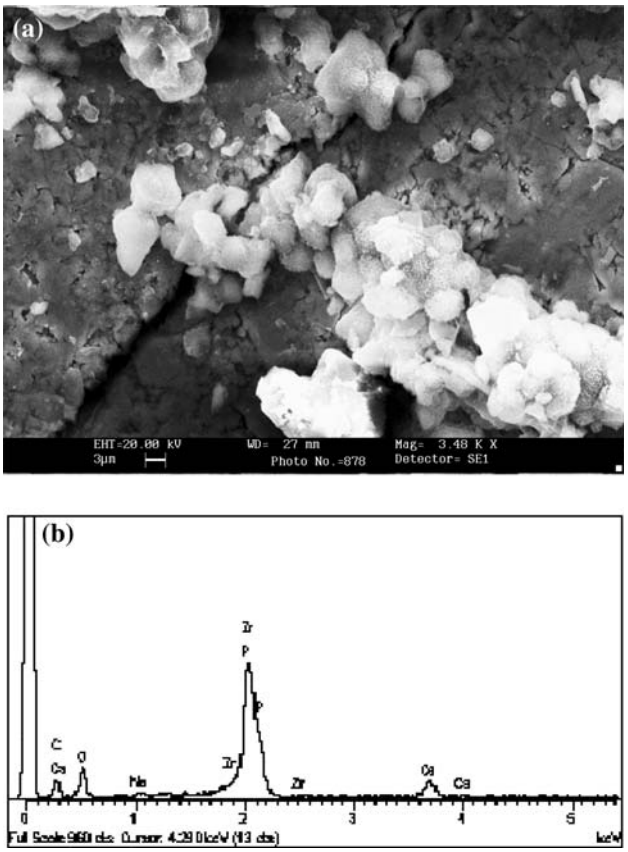

Fig. 9 (**a**) SEM spectra of PCL/ZrO_2-5 wt%Y_2O_3 gel 6 wt%, samples after 21 days of exposed to SBF (**b**) corresponding EDS spectrum

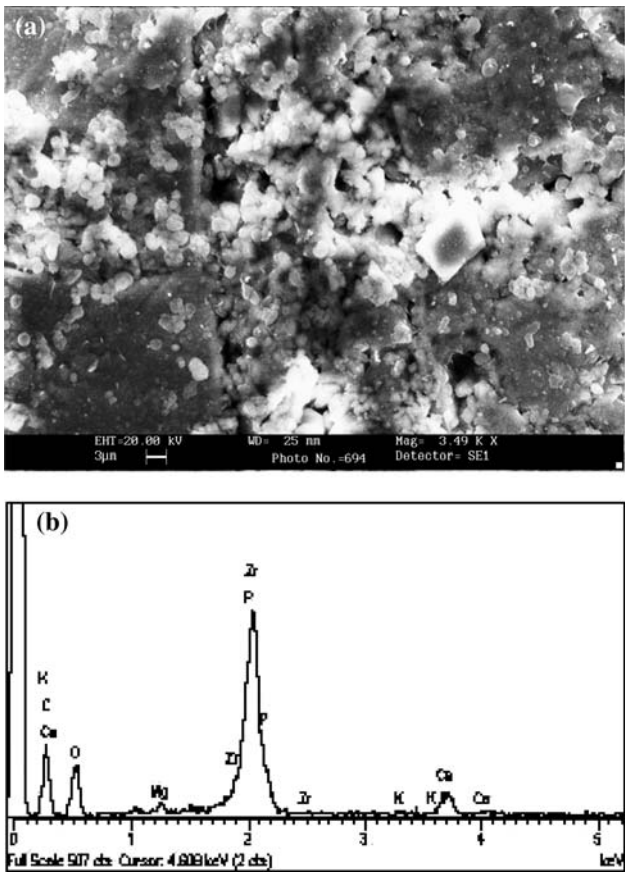

Fig. 10 (**a**) SEM spectra of PCL/ZrO_2-5 wt%Y_2O_3 gel 12 wt%, samples after 21 days of exposed to SBF (**b**) corresponding EDS spectrum

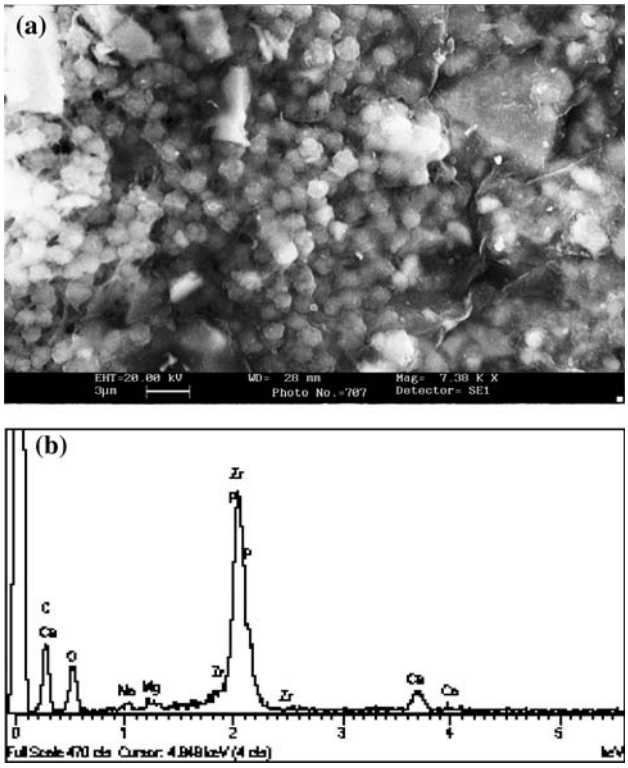

Fig. 11 (**a**) SEM spectra of PCL/ZrO_2-5 wt%Y_2O_3 gel 24 wt%, samples after 21 days of exposed to SBF (**b**) corresponding EDS spectrum

and aliquots of 600 µL were withdrawn at 1-h interval and replaced with an equal volume of release medium pre-equilibrated to temperature. Released ampicillin was assayed by measuring the photometrical absorbance at 197 nm. In order to establish the relationship between the UV absorbance of sodium ampicillin at λ = 197 nm, and the concentration of the sodium ampicillin solution, a calibration curve (r^2 = 0.9907), Fig. 12, was drawn for a standard solution of sodium ampicillin with four levels of concentration: 0.0 mM, 1.0 mM, 2.0 mM and 3.0 mM. All the standard solutions were prepared in SBF.

Figure 13 shows the drug release rates expressed as a percentage of the drug delivered, related to the drug-loading value, as a function of time.

It was observed that from the ZrO_2-5 wt%Y_2O_3 + PCL6 wt% + AMP5 wt% gel, the amount of ampicillin was released in a relatively fast manner during the initial 6 h (about 60%wt) and it seems to be completed within 180 h (about 7 days), while the amount of ampicillin released from the ZrO_2-5 wt%Y_2O_3 + PCL12 wt% + AMP5 wt% is quite lower than ZrO_2-5 wt%Y_2O_3 + PCL6 wt% + AMP5 wt% during the initial 6 h (about 35 wt%) but the drug is released completely within 200 h (about 8 days). There is not most evident difference in the time of release. For the ZrO_2-5 wt%Y_2O_3 + PCL24 wt% + AMP5 wt% the drug released during the initial 6 h is about 40 wt%, faster than ZrO_2-5 wt%Y_2O_3 + PCL12 wt% and slower than ZrO_2-5 wt%Y_2O_3 + PCL6 wt%, and it is complete in about two weeks.

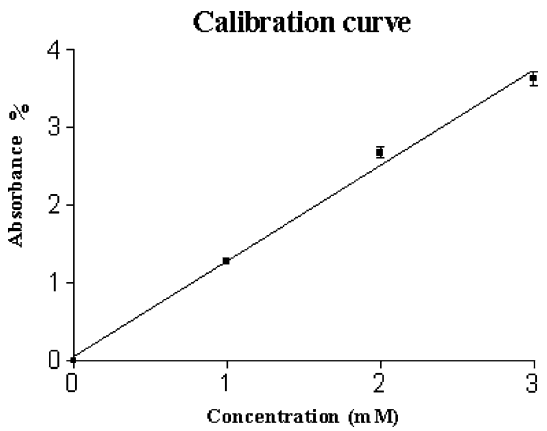

Fig. 12 Calibration curve UV absorbance of sodium ampicillin (r^2 = 0.9907)

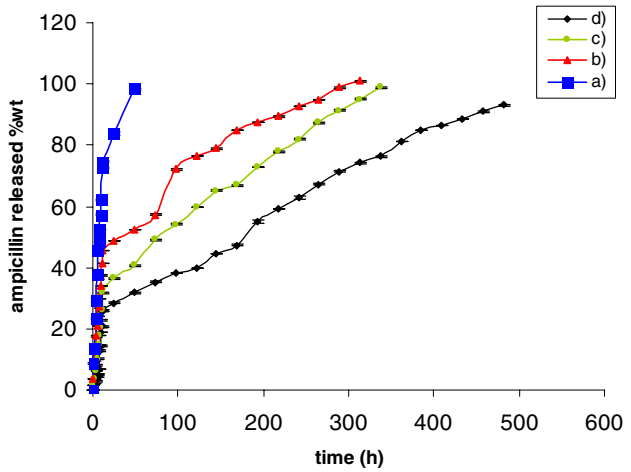

Fig. 13 Time-dependent drug release plot for PCL/ZrO_2-5 wt%Y_2O_3. (**a**) ZrO_2-5 wt%Y_2O_3 Amp5%; (**b**) ZrO_2 -5 wt%Y_2O_3 PCL6%Amp5%; (**c**) ZrO_2-5 wt%Y_2O_3 PCL12%Amp5%; (**d**) ZrO_2-5 wt%Y_2O_3 PCL24%Amp5% at 37 °C in SBF solution

The differences observed in the release behaviour of the ampicillin from ZrO_2-5 wt%Y_2O_3 + PCL(6, 12 and 24 wt%) + ampicillin 5 wt% might be due to the different networks of the three gels that determined the different content percentage of PCL.

The two stage release observed in all cases suggests that the initial stage of release occurs mainly by dissolution and diffusion of the drug entrapped close to or at the surface of the samples. The second and slower release stage was thought to involve the diffusion entrapped within the inner part of the clusters.

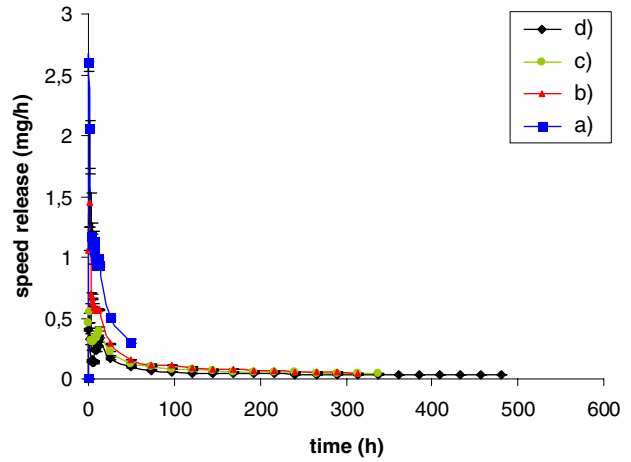

Fig. 14 Time-dependent drug release rate plot for PCL/ZrO_2. (**a**) ZrO_2-5 wt%Y_2O_3 Amp5%; (**b**) ZrO_2 -5 wt%Y_2O_3 PCL6%Amp5%; (**c**) $ZrO_2Y_2O_35$%PCL12%Amp5%; (**d**) ZrO_2-5 wt%Y_2O_3 PCL24%Amp5% at 37 °C in SBF solution

An interesting observation is the general presence of a lag period, which is indicative of the need for solvent penetration into the structure.

Figure 14, shows this particular kinetic describing the changes of the release speed during the two stages.

Conclusions

The polycaprolactone/Zirconium (PCL/ZrO_2-5 wt%Y_2O_3) material, prepared via sol–gel process, was found to be an organic/inorganic hybrid material.

The polymer (PCL) was incorporate into network by hydrogen bonds between the carboxylic groups of organic polymer and the hydroxyl groups of inorganic matrix. The formation of hydrogen bonds was ascertained by FTIR measurements. Moreover the AFM and SEM analysis confirm that the PCL/ZrO_2-5 wt%Y_2O_3 can be considered a homogenous organic/inorganic hybrid material because the average domains are less than 400 nm in size.

Finally the formation of a layer of hydroxyapatite on the surface when samples of the PCL/ZrO_2 were soaked in SBF (fluid simulating body) showed by SEM micrograph and related EDS, indicates that the PCL/ZrO_2 can be considered a bioactive material.

Further investigations are required for evaluating the mechanical properties of the synthesized hybrid material.

References

1. C. SANCHEZ and F. RIBOT, in *Proceedings of the First European Workshop on Hybrid organic–inorganic Materials (Synthesis, Properties, Applications)*, Bierville-France, (1993).
2. *Hybrid Organic–inorganic Materials* edited by L.L KLEIN and C. SANCHEZ Special Issue of J. Sol–Gel Sci. Tech. **5** (1995)
3. C. SANCHEZ and F. RIBOT, *New. J. Chem.* **18** (1994) 1007
4. P. JUDEINSTEIN and C. SANCHEZ, *J. Mater. Chem.* **6** (1996) 511
5. L. L HENCH and J. K. WEST, *Chem. Rev.* **90** (1990) 33
6. B. M. NOVAK, *Adv. Mater.* **5** (1993) 422
7. G. H. HSIUE, J. K. KUO, R. J. JENG, J. I. CHEN, X. L. JIANG, S. MARTURUNKAKUL, J. KUMAR and S. K. TRIPATHY, *Chem. Mater.* **6** (1994) 884
8. Y. WEI, J. XU, H. DONG, J. H. DONG, K. Y. QIU and S. A. JANSON-VARNUM, *Chem. Mater.* **11** (1999) 2023
9. C. J. BRINKER and G. W. SCHERER, 1989, in Sol–Gel science, the physics and chemistry of Sol–Gel processing (San Diego: Academic Press)
10. L. C. KLEIN, 1988, in Sol–Gel technology (Park Ridge NJ: Noyes PublicaZrons)
11. I. A. DAVID and G. W. SCHERER, *Chem. Mater.* **7** (1995) 195
12. J. J. FITZGERALD, C. J. T. LANDRY and J. M. POCHAN, *Macromolecules* **25** (1992) 3715
13. T. SAEGUSA, *Macromol. Symp.* **98** (1995) 719
14. M. CATAURO, M. G. RAUCCI, F. DE GAETANO and A. MAROTTA, *J. Mater. Sci.* **38** (2003) 3102
15. M. CATAURO, M. G. RAUCCI, F. DE GAETANO, A. BURI, A. MAROTTA and L. AMBROSIO, *J. Mater. Sci.* **38** (2004) 991

16. T. KOKUBO, H. -M. KIM and M. KAWASHITA, *Biomaterials* **24** (2003) 2161
17. T. KOKUBO, 1999, Boll. Soc. Esp. Ceram.Vid.,in *Proceedings of the XVI Int. Cong. on Glass*, Madrid, 1992, **1(31-C1),** 119
18. C. OHTSUKI, T. KOKUBO and T. YAMAMURO, *J. Non - Cyst. Solids* **143** (1992) 84
19. L. L. HENCH and D. E. CLARK, *J. Non-Cryst. Solids* **28** (1978) 83
20. A. PAUL, 1990, in *Chemistry of glasses*, 2nd edn (London, New York: Chapman and Hall) p. 184
21. D. S. BANSAL and C. G. PANTANO, *Non-Cryst. Solids* **115** (1992) 147
22. M. THOMAS, 1996, in *Ultraviolet and Visible Spectroscopy*, 2nd edn, edited by D.J. ANDO (England: Wiley) pp. 16–30.
23. C. SANCHEZ, J. LIVAGE, M. HENRY and F. BABONNEAU, *J. Non-Cryst. Solids* **100** (1988) 650
24. E. RADLEIN and G. H. FRISCHOT, *J. Non-Crist. Solids* **222** (1997) 69
25. Y. WEI, J. DANLIANG, D. BRENNAN, D. N. RIVERA, Q. ZHUANG, N. J. DI NARDO and K. QIU, *Chem. Mater.* **10** (1998) 769